JOURNAL OF MATERIALS SCIENCE **40** (2005) 1929–1935

A thermal imaging technique for studying crack development in wood under torsional loading

ZHENG CHEN
University of New Brunswick, Fredericton, NB, Canada
E-mail: cxc620@yahoo.ca

B. GABBITAS
University of Waikato, Hamilton, New Zealand

D. HUNT
London South Bank University, London, UK

A thermal imaging system has been used for monitoring fracture in wood under both static and fatigue torsional loading. The thermal images of softwood test-pieces containing a knot under torsional loading predicted the cracking time and crack position that agreed well with visual observation. The thermal images obtained under torsional fatigue loading indicated a temperature increase during the unloading part of a loading cycle, which meant that thermal energy was dissipated during the relaxation stage of the loading cycle. The maximum temperature reached also increased as the loading cycles increased. Results from thermal images of a softwood indicated that the earlywood exchanged more thermal energy than latewood. Optical microscopy and SEM confirmed that in earlywood the region near a growth ring is the weaker area. For all the test pieces, whether softwood or hardwood, with or without a knot, the hotspots revealed during thermal imaging appeared before the load dropped sharply and these were confirmed to be the positions for crack initiation. This shows that it is possible to predict and depict failure and its progress using thermal imaging techniques.

1. Introduction

It is known that when wood test pieces are loaded either statically or under fatigue conditions, there will be a change of stored energy when the test-pieces are loaded, unloaded, starting to fail or failing by the nucleation, development and propagation of flaws [1]. It has been reported that there is a decrease in the hysteresis energy during the cyclic torsional testing of both softwood and hardwood [2] and that some of this energy is dissipated as surface and sound waves when the test pieces are loaded in bending, torsion or tension [2–5]. The released energy deriving from microcracking will cause a small increase in the temperature of the test-piece. According to the Plank radiation law [6], a certain amount of emitted energy will be at a maximum level in the thermal region of the electromagnetic spectrum. This invisible radiation can be detected by a thermal camera and the information about the temperature distribution in this area at a given instant can be measured and shown as a thermal image, with different colour distributions corresponding to the temperature distribution. By measuring the temperature distribution in a thermal image at a given instant, significant changes taking place in the wood, such as localised hot spots at places where microcracks are forming, can be monitored.

The thermal phenomenon can also be described by the heat conduction equation [7]:

$$\rho C_\alpha \dot{T} + \operatorname{div} q = D_1 + r + \rho T \frac{\partial^2 \psi}{\partial \alpha_j \partial T} \dot{\alpha}_j, \quad (1)$$

where,

ρ: the mass density
C_α: the heat capacity when (α_j) $j = 1, \ldots, n$
α_j: internal state variables ($j = 1, \ldots, n$). If the load is in elastic stage, $\alpha_1 = \varepsilon_e$ (an elastic strain tensor)
q: the heat influx
r: the external heat supply
D_1: the intrinsic dissipation; or heat source.
ψ: the specific free energy ψ (T, α_j)
T: absolute temperature
$D_1 \rho T \frac{\partial^2 \psi}{\partial \alpha_j \partial T} \dot{\alpha}_j$: the dissipation energy associated to the state variables (α_j), $j = 1, \ldots, n$

So in the elastic stage, the dissipation energy will change as the elastic strain tensor ε_e changes. During elastic loading there is an increase in α_j which leads to a decrease in the dissipation energy and a temperature decrease. When a material loses elastic strain energy at locations where cracking begins, the internal state

variable α_j decreases and this causes a localized temperature increase. This energy conversion changes the thermal radiation emitted from the sample.

The early thermal imaging technology was mostly used in military applications after the first infrared detector appeared in 1830 [8]. With advances in technology in the 1990s, particularly in thermal imaging systems when high-resolution focal plane arrays (FPAs) and uncooled FPAs were introduced, the applications for thermal imaging systems have been developed into the other areas such as the method of determining the spatial distribution of heat in objects, material inspection by monitoring temperature disturbance caused by defects, and nondestructive testing where heat is applied in a periodic fashion, etc. [9].

The main thermography methods for NDT are called pulse [10–12], heating up and lock-in [13] thermography. Using lock-in thermography, Sembach *et al*. [14] detected 19 mm wide drilled slots at a depth of 4–5 mm beneath the surface of medium density fibre boards and chip boards respectively, and were able to separate badly laminated from correctly laminated chipboard. Wu and Busse [15] detected 4 mm diameter holes beneath the substrate of different wood species, and knots in the substrate beneath a 2 mm thick veneer with the same methods. Using heating up thermography Xu *et al.* [16] detected 0–50 mm large areas without glue with a contrast up to 0.7°C beneath 1.3–3 mm thick surface layers of white Seraya. Berglind and Dillenz [17] also detected the glue deficiency in laminated wood with this technology. All these methods above need controlled heat injection to produce radiation.

Some research using thermal imaging without heat injection has been done by Chrysochoos *et al.* [7, 18] who have studied the localization mechanism in steel under static and fatigue tensile loading. They used a thermal camera to monitor the testing process directly without heat injection. They observed the release of the stored energy or heat dissipation during elastic unloading (reversible path), or after deformation [18]. Using infrared thermography and speckle techniques, they determined a link between the distribution of heat sources and the strain rate fields on the surface of steel samples during monotonic tensile tests [19]. Bardet [20] used the same thermal imaging technology for monitoring the energy changes in wood under cyclic tensile loading. She reported that the dissipation of thermal energy would decrease with an increase in cycle number and decrease in deformation rate. This information provided a basis for a research programme to use thermal imaging techniques to monitor and identify the effects of defects such as knots, localized changes in grain orientation and other structural discontinuities on the fracture process during static and torsional fatigue loading.

2. Materials and testing methods

A thermal imaging camera was used to monitor crack nucleation and propagation during torsional loading. Initially the effect of knots on the fracture of the softwood, Scots Pine was investigated using round cross-section test-pieces 20 mm diameter and 200 mm long (Fig. 1). An AGEMA-880 thermal camera connected to a computer was used in the early stages of this research. The distance between the sample and camera was set at either 190 mm or 500 mm and the thermal camera speed was 2 pictures per second. The test-pieces were coated with oil gloss grey paint with a high emissivity at 20°C. A DARTEC tensile testing machine was used for the preliminary work with an attached rig (Fig. 2), which adapted the tensile operation of the equipment to give torsional loading [2]. In later experimental work a special portable rig for applying torsional loading was designed. The design of this rig comprised a square cross-section sample grip fixed to the bed frame with the other grip connected to a moving arm. The moving arm derived its motion from a connecting arm attached to an eccentric wheel on a motor at one end and to the bed frame through a bearing at the other end. A slot in the moving arm made the arm's connecting point movable in order to change the load. A strain gauge proving ring in the middle of the connecting arm was used to measure the load during the test. In this later work, hardwood (Red Lauan) and softwood (Sitka Spruce) test-pieces with a rectangular cross-section were used. This made it easier to capture the thermal images during torsional loading. For the later experimental work a faster thermal camera CEDIP was used for imaging. The camera speed was set at 30 pictures per second and 150 pictures per second. The distance between the sample and camera was 500 mm. The change of load with time during tests using the two camera speeds were monitored and recorded by computer and XY recorder and the data was processed using a programme written with MATLAB software.

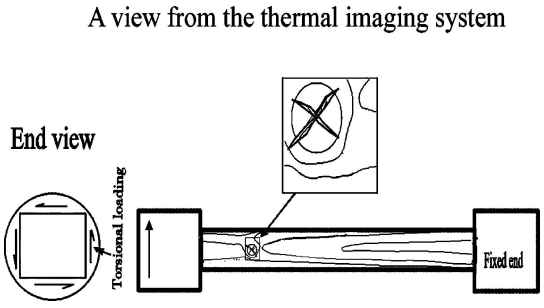

Figure 1 A diagram of the test-piece shape and the area viewed during static torsional testing of a softwood containing a knot.

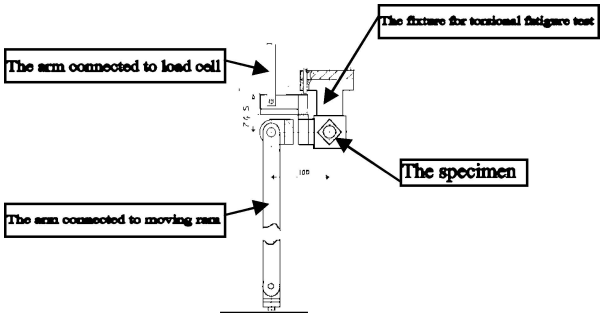

Figure 2 The arms of the fixture connected to the moving ram and load cell of a DARTEC tensile testing machine.

3. Results

3.1. Monitoring the static torsional testing of a softwood containing a knot using an AGEMA-880 thermal imaging system

Captured thermal image data for increasing times after loading commenced are shown in Figs 3, 4 and 5 in order of increasing time. The scale of these pictures is 16:1, and the legend to the right of these pictures is absolute temperature. The load speed was set at 0.5 degrees of twist angle per second. These figures show that when a crack appears, there is a temperature change around part of the knot. It has been confirmed that the

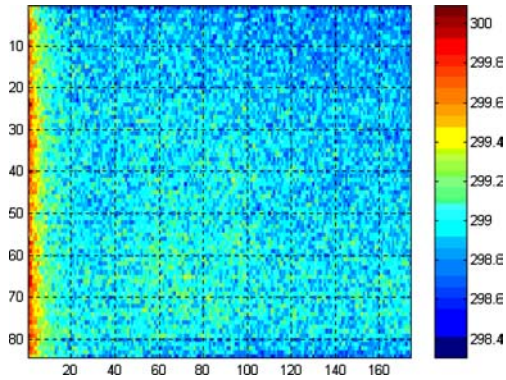

Figure 3 Thermal image of a softwood with a knot under static torsional loading after loading for 6 s. The spectrum to the right is in absolute temperature.

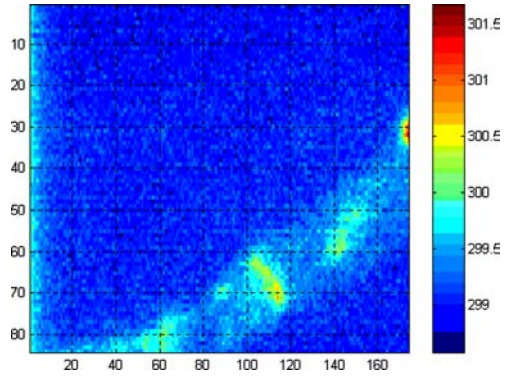

Figure 4 Thermal image of a softwood with a knot under static torsional loading after loading for 8 s. The spectrum to the right is in absolute temperature.

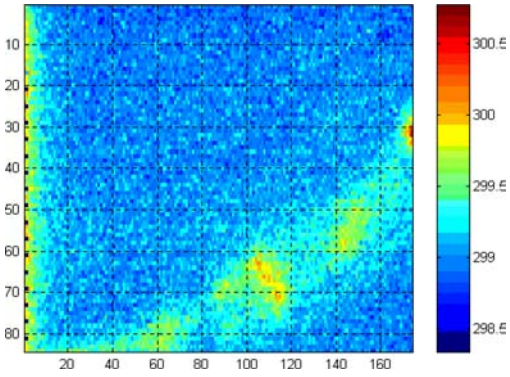

Figure 5 Thermal image of a softwood with a knot under static torsional loading after loading for 8.5 s. The spectrum to the right is in absolute temperature.

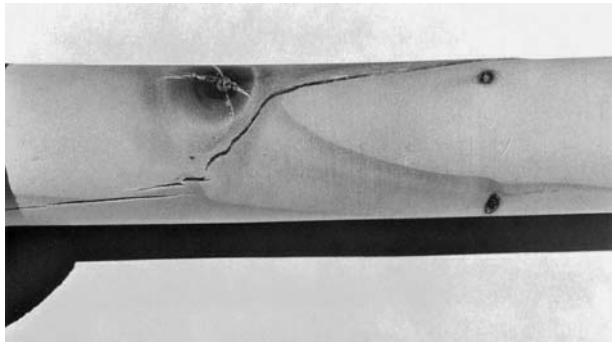

Figure 6 A softwood testpiece containing a knot showing the crack path around the knot.

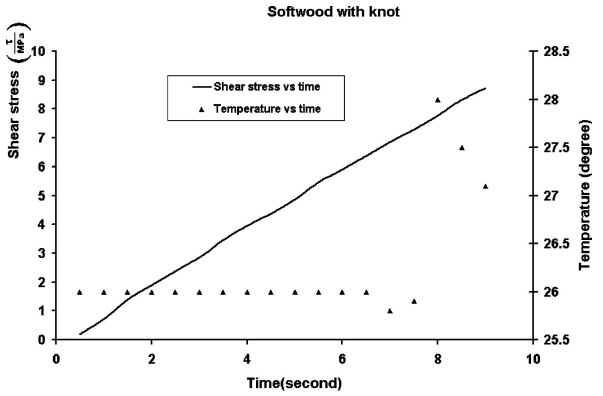

Figure 7 The temperature produced by thermal radiation and the shear stress as a function of testing time, for the static torsional loading of a softwood with a knot.

position where the temparature change occurred corresponds with the location of cracking (Fig. 6). These thermal images provide information that visualises the process of crack initiation and development under torsional loading.

The temperature at the point (115,70) within the cracked area in Figs 3–5 has been measured. The changes in temperature and shear stress in the test-piece with increasing time is shown in Fig. 7. There is a small temperature increase when the test-piece is loaded and when a crack appears, the temperature of the measured point increases more. This phenomenon confirmed that there is some thermal energy dissipation during loading and cracking of the test-piece. The dissipating thermal energy belongs to the energy that is released when the material fails or starts to fail by the nucleation, development and propagation of flaws. Both Figs 6 and 7 show that a torsional crack forms, with an orientation at 30°–60° with the twist axis, at the interface between a knot and the clear wood.

3.2. Thermal imaging experiments for a hardwood test-piece having a 0° grain angle (parallel to the twist axis) and loaded in static torsion

Figs 8, 9 and 10 show the fracture process in a hardwood test-piece under torsional loading. The load speed was set at 5.2 degrees of twist angle per second. At the start of loading a "hot-spot" at coordinate position (115, 75) appeared (Fig. 8). The position of the

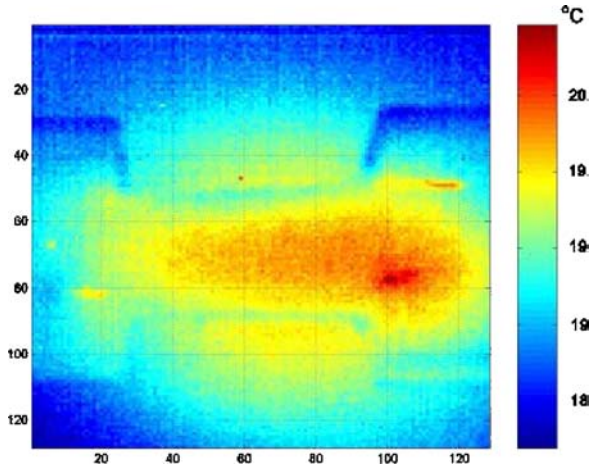

Figure 8 Thermal image of a hardwood with a 0° grain angle under static torsional loading after loading for 2.833 s. Picture scale: 3.2:1. The temperature spectrum to the right is in Celsius.

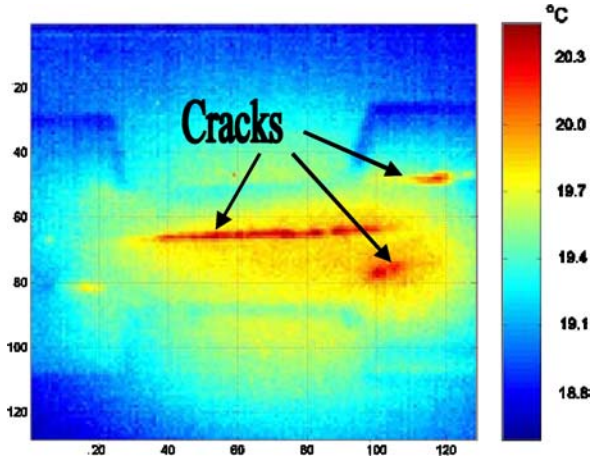

Figure 9 Thermal image of a hardwood with a 0° grain angle under static torsional loading. Testing has run 2.867 s. Picture scale: 3.2:1. The temperature spectrum to the right is in Celsius.

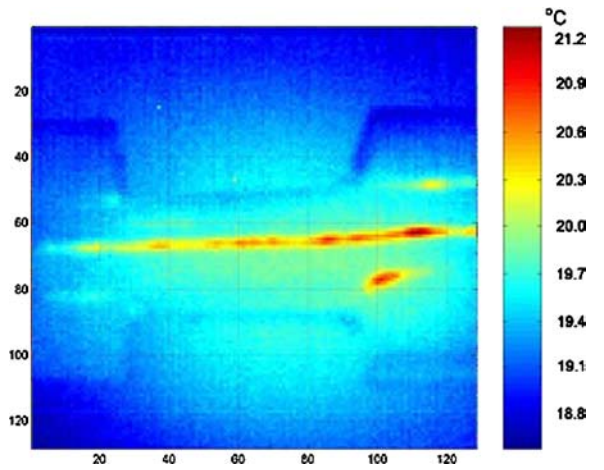

Figure 10 Thermal image of a hardwood with a 0° grain angle under static torsional loading. Testing has run 3.167 s. Picture scale: 3.2:1. The temperature spectrum to the right is in Celsius.

"hot-spot" shown in Fig. 10 corresponded with the position of crack nucleation. A comparison of the curve of temperature versus time with the curve of shear stress versus time (Fig. 11) shows that before the load reaches a maximum level, the temperature of the "hot-spot" has

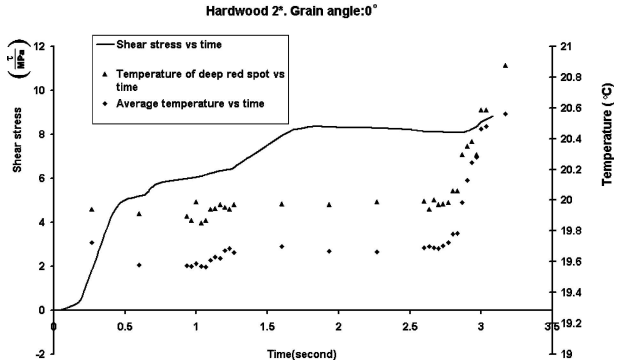

Figure 11 The temperature of the deep red spot, the average temperature produced by thermal radiation and shear stress as a function of testing time for static torsional testing of hardwood with a 0° grain angle. The points at time 0.25 s and 3 s indicate crack nucleation.

increased. This abrupt increase in the temperature of the "hot-spot" with time indicates crack initiation well before final failure.

It indicates that the thermal behaviour observed here presages the crack nucleation. Fig. 11 also compares average temperature with the temperature of the deep red spot in Figs 8–10 with increasing time. This shows that the temperature in the position where the cracking begins is higher than the average temperature from the start of the test. So the thermal imaging also foretells the site of crack development.

3.3. Thermal imaging experiments for a softwood test-piece having a 45° grain angle and loaded in static torsion

For a softwood with a 45° grain angle, the positions in the earlywood where the temperature was measured are the points (85, 60) and (95, 60) in Figs 12–14. The cracking position where the temperature was measured is the point (115, 60) in Figs 12–14. The temperatures of both the earlywood, the position where cracking occurred and shear stress values, respectively, versus time have been plotted in Fig. 15. The load speed was set at 2.6 degrees of twist angle per second. It shows that there is more thermal energy radiating from the earlywood part of the growth ring than in the latewood before

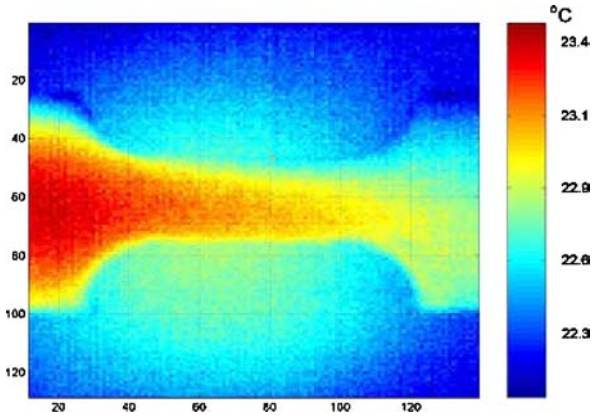

Figure 12 Thermal image of a softwood with a 45° grain angle under static torsional loading. Testing has run 0.333 s. Picture scale: 3.0:1. The temperature spectrum to the right is in Celsius.

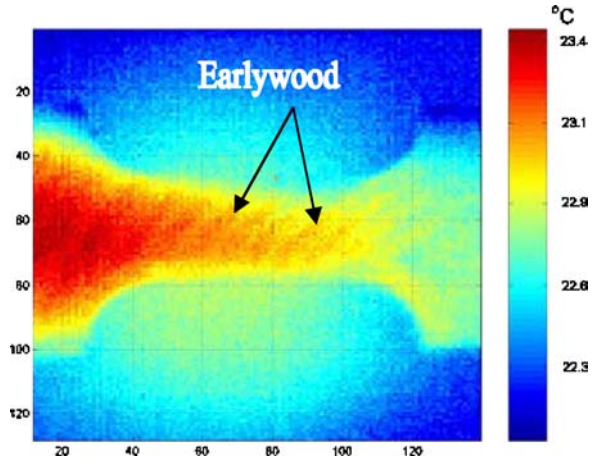

Figure 13 Thermal image of a softwood with a 45° grain angle under static torsional loading. Testing has run 1.140 s. Picture scale: 3.0:1. The temperature spectrum to the right is in Celsius.

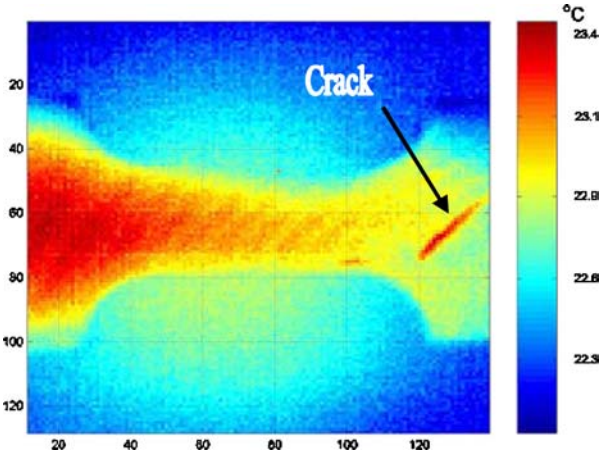

Figure 14 Thermal image of a softwood with a 45° grain angle under static torsional loading. Testing has run 1.193 s. Picture scale: 3.0:1. The temperature spectrum to the right is in Celsius.

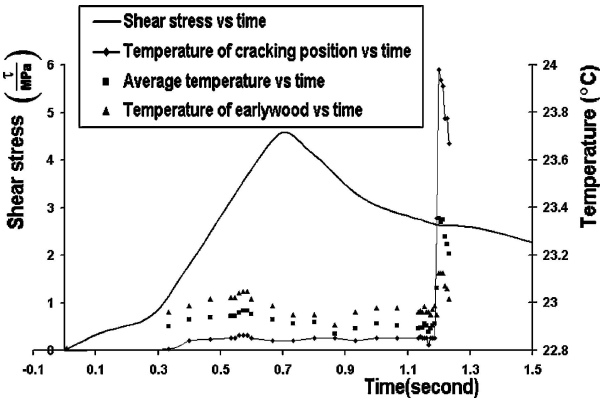

Figure 15 The temperature at the cracking position, the temperature in the earlywood, the average temperature produced by thermal radiation and shear stress as a function of testing time for static torsional loading of the softwood with a 45° grain angle.

the crack appears. Observations of the softwood test-piece, after torsional loading, using Scanning Electron Microscopy showed that cracks tend to form in the earlywood near a growth ring (Fig. 16). Since the sample's face was not perfectly normal to the thermal imaging direction during testing, the thermal imaging system

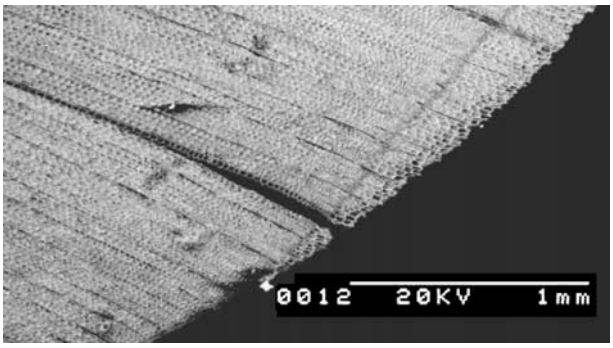

Figure 16 SEM photo of the cross-section of a softwood that has been tested under static torsional loading.

detected more dissipation energy in the sample's left side than the right side as shown in Figs 12–14. The cracking position was just at the right hand side of the sample. Consequently the temperature at this position is lower than the average temperature for most of the time before the load reaches its maximum level. But Figs 12–14 still show that cracking takes place in the earlywood.

3.4. Thermal imaging experiments for a hardwood test-piece having a 45° grain angle and loaded in cyclic torsion

Fig. 17 shows the change in average temperature versus test time compared with changes in shear stress with time for a hardwood having a 45° grain angle. The rate of load cycling was always less than 32 cycles per minute (0.53 Hz) under unidirectional (pulsating) load with twist angle control mode. The twist angle for each cycle test was 4.2° . The temperature was measured at point (25, 60) in Figs 18–20 where a "hot spot" appeared and which eventually developed into a crack. It indicates that there is a large temperature increase which presages cracking, in the cycle before cracks are observed. It also indicates that the temperature will go down when the sample is loaded and will rise when the sample is unloaded. The maximum temperature for each load cycle will increase with cycle number before cracking takes place, which means that with increasing cycles, more thermal energy is dissipated. This result

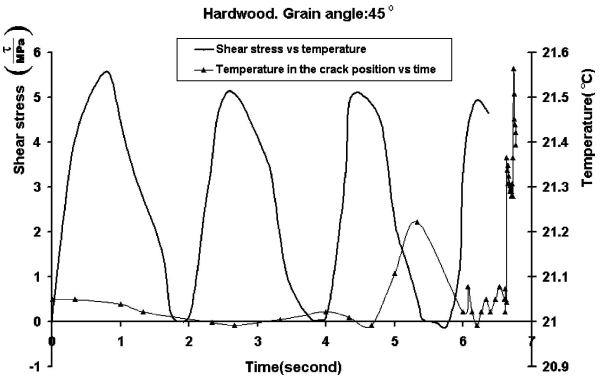

Figure 17 The temperature in the crack position produced by thermal radiation and the shear stress as a function of testing time for cyclic torsional loading of the hardwood with a 45° grain angle.

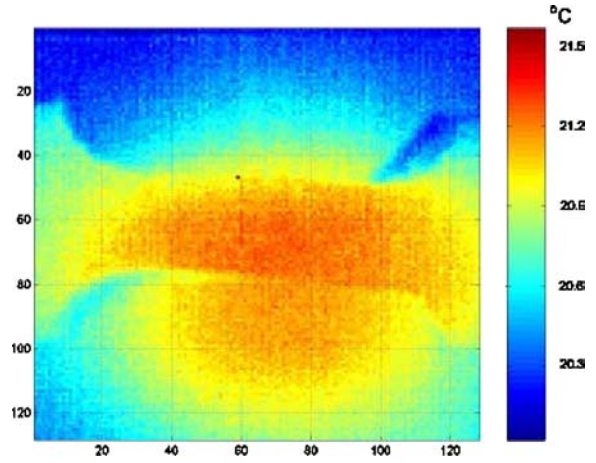

Figure 18 Thermal image of a hardwood with a 45° grain angle under cyclic torsional loading. Testing has run 1.333 s and is in the first loading cycle. Picture scale: 3.0:1. The temperature spectrum to the right is in Celsius.

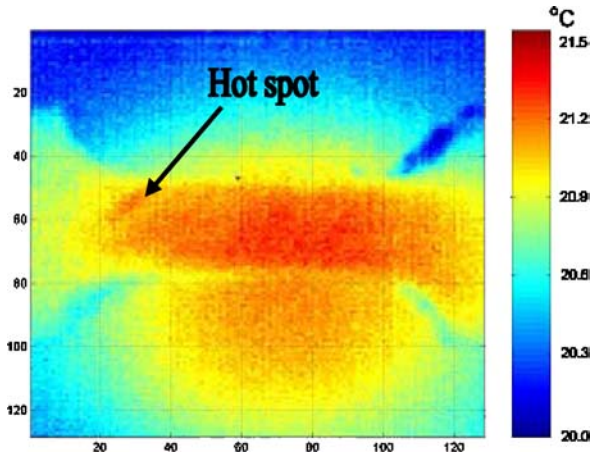

Figure 19 Thermal image of a hardwood with a 45° grain angle under cyclic torsional loading. Testing has run 5.333 s and the specimen is just unloaded from the third loading cycle. Picture scale: 3.0:1. The temperature spectrum to the right is in Celsius.

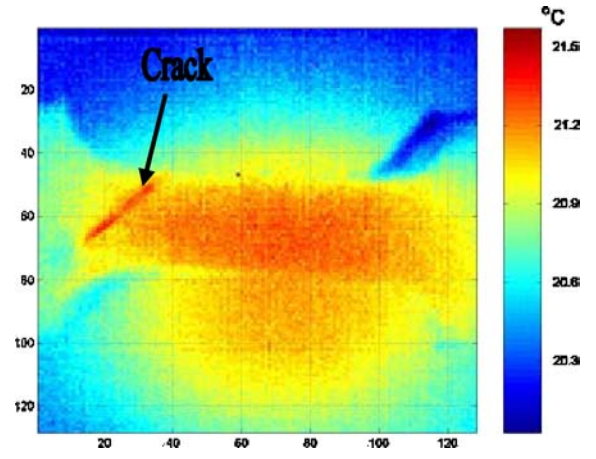

Figure 20 Thermal image of a hardwood with a 45° grain angle under cyclic torsional loading. Testing has run 6.666 s and a crack has propagated. Picture scale: 3.0:1. The temperature spectrum to the right is in Celsius.

agrees with those obtained from test monitoring using acoustic emission, where the acoustic energy dissipated from the sample will increase with cycle number when failure approaches [2].

TABLE I The influence of various factors on the localised temperature changes in wood under torsional loading

Factors influencing the temperature produced by the thermal radiation from the test-piece surface	Temperatures change +: Temperature increase −: Temperature decrease
Elastic loading	−
Elastic unloading	+
Internal friction	+
Crack propagation	
Friction due to rubbing	+
Unloading	+
Microcracking	+

4. Discussion

Using a thermal imaging approach, the influence of various factors on localised temperature changes is summarised in Table I. It shows that elastic unloading, internal friction, microcracking, relaxation unloading and crack propagation will lead to a temperature increase, whereas elastic loading and relaxation loading will result in a temperature decrease.

For both the softwoods with and without a knot during static loading, before a maximum load is reached, the localised temperature at the crack position decreases or remains constant and then sharply increases as cracking begins (Figs 5, 7, 11 and 15). It is well known that the formation of a crack leads to an overall elastic-energy decrease. The heat conduction Equation 1 shows that the value of the internal state variables α_j increases during elastic loading (in the same way that the elastic strain tensor ε_e increases when the sample is loaded), which results in a decrease in the dissipation energy. As a consequence the local temperature of a test-piece at the crack will decrease. After cracking, the internal state variables α_j will decrease strongly (the strain tensor ε_j and internal state variables will decrease strongly). So the dissipation energy will increase and the surface temperature of the sample rises. The value of the temperature increase after cracking has occurred will be much bigger than the value of the temperature decrease before cracking, because the value of the increase in the tensor ε_j and other internal state variables during a steadily increasing load, are relatively much smaller than the reduction in the values of the internal state variables during cracking. So the relatively large increase in temperature during or after cracking can be used to determine whether any cracking has taken place.

Persson [21] listed the elastic parameters for earlywood and latewood in the softwood, Norway Spruce. His data shows that latewood has a higher stiffness than earlywood, which means that latewood needs more energy than earlywood to achieve the same strain. This will make the internal state variables α_j in Equation 1 for latewood higher than those for earlywood, so that latewood dissipates less energy than earlywood. This is why the earlywood shows a larger temperature increase than latewood during torsional loading (Figs 13–14). For hardwood, it is probable that the stiffness difference between earlywood and latewood is small, so the temperature difference for earlywood

and latewood is not so discernible during torsional loading.

For test-pieces under cyclic torsional loading, the surface temperature of a sample changes in two ways. On the one hand, the temperature will decrease and increase as samples are loaded and unloaded elastically at each loading cycle (Fig. 17). A similar phenomenon has been reported by Bardet [20] during the tensile fatiguing of wood. This can be explained by Equation 1 because an increase and a decrease in the internal state variables α_j leads to a temperature decrease and increase. On the other hand, the maximum temperature of each cycle increases with increasing cycle number, possibly because of a relaxation of the sample, or internal friction. This will cause the internal state variable α_j to reduce and the dissipation energy increase.

Since the temperature increase often happens when the sample is unloaded, the onset time for a localised temperature increase always lags behind the actual onset time for crack nucleation and propagation. This method can be used for recording the process of failure and to determine the position of the crack. But this method cannot record or predict the actual time of failure. Comparing this method with the acoustic emission (AE) technique it should be noted that the AE can record the onset time of crack nucleation but cannot record the position of the crack [2].

5. Conclusions

1. In static torsional testing of wood, the temperature change produced by thermal radiation will decrease a little when a sample is loaded but increase quickly after cracking takes place. The thermal imaging picture can display the origin of crack nucleation and the progress of crack propagation. The thermal imaging of softwood indicated that earlywood exchanged more thermal energy than latewood. It is confirmed by SEM that earlywood near the growth ring is the weaker area.

2. The thermal imaging of softwood containing knots shows that there is a change of temperature distribution around the areas of crack formation during failure. The areas of temperature change corresponded to the crack position.

3. The thermal imaging of wood under torsional fatigue loading shows that the temperature will decrease when the sample is loaded and it will increase when the sample is unloaded. The maximum temperature reached will increase with loading cycle, which means that there is thermal energy dissipation during the relaxation stage. The crack position will dissipate more thermal energy than other places in the early cycles before the loading cycle which leads to failure. The thermal imaging of softwood under cyclic torsional loading also showed that the earlywood dissipated more energy than latewood.

4. The hot spots in both softwood and hardwood under static or fatigue torsional loading were confirmed to be cracking positions. This shows that it is possible to predict failure using thermal imaging.

Acknowledgements

The authors' prime debt of gratitude go to the people at Montpellier University, France, particularly to thank Dr Joseph Gril, Professor André Chrysochoos for their help with the thermal imaging work. We also like to thank Dr Peter Bonfield and the Building Research Establishment in UK for their providing the wood materials, and giving useful suggestions for this project.

References

1. V. BUCUR, in "Acoustics of Wood" (CRC Press, Boca Raton, New York, USA, 1995) p. 221.
2. Z. CHEN and B. GABBITAS, in First international conference of the Europe Society of Wood Mechanics, Lausanne, Switzerland, 19–21 April, 2001, p. 393.
3. R. W. RICE and C. SKAAR, *Wood Sci. Techn.* **24** (1990) 123.
4. D. WU and G. BUSSE, *TAPPI 1995 Europ. Plast. Lamin. Symp.* **79**(8) (1995) 119.
5. G. DILL-LANGER and S. AICHER, in Proceedings of COST Action E8 on Wood and Wood Fiber Composites, Stuttgart, Germany, 13–15 April, 2000, p. 93.
6. S. G. BURNAY, T. L. WILLIAMS and C. H. JONES, in "Applications of Thermal Imaging" (Hilger Ltd., Bristol, UK, 1988) p. 1.
7. A. CHRYSOCHOOS, O. MAISONNEUVE, G. MARTIN, H. CAUMON and J. C. CHEZEAUX, *Nucl. Engns. Design* **114** (1989) 323.
8. G. GAUSSORGUES, in "Infrared Thermography" (Chapman & Hall, University Press, Cambridge, UK, 1994) p. xv.
9. V. P. VAVILOV, in "Subjective Remarks on the Terminology used in Thermal/Infrared Nondestructive Testing" in Thermosense XVIII, edited by D. D. Burleigh and J. W. M. Spicer, *SPIE Proc.*, **2766** (1996) 276.
10. W. N. REYNOLDS and G. M. WELLS, *Brit. J. NDT* **26**(1) (1984) 40.
11. S. K. LAU, D. P. ALMOND and J. M. MILNE, *NDT Eval. Intern.* **24**(4) (1991) 195.
12. R. L. THOMAS, L. D. FAVRO, P. K. KUO, T. AHMED, X. HAN, L. WANG, X. WANG and S. M. SHEPARD, in Proceedings of 15th International Congress on Acoustics, Trondheim, Norway, June 26–30, 1995 p. 433.
13. G. BUSSE, D. WU and W. KARPEN, *J. Appl. Phys.* **71**(8) (1992) 3962.
14. J. SEMBACH, D. WU, A. SALERNO, G. HORA and G. BUSSE, in Proceedings of Workshop on Nondestructive Testing of Panel Products, Llandudno, UK, 11 October, 1997 (J. Hague 1997) p. 41.
15. D. WU and G. BUSSE, in *TAPPI 1995 Europ. Plast. Lamin. Symp.* **79**(8) (1995) 119.
16. Y. XU, S. OKUMURA and M. NOGUCHI, *Mukuzai gakkaishi-J.* **39**(5) (1993) 544.
17. H. BERGLIND and A. DILLENZ, in 12th International Symposium on Nondestructive Testing of Wood, Sopron, Hungary, 2000 p. 413.
18. A. CHRYSOCHOOS and F. BELMAHJOUB, *Arch. Mech.* **44** (1992) 55.
19. A. CHRYSOCHOOS, H. LOUCHE, J. M. MURACCIOLE, M. NÉMOZ-GAILLARD, J. L. SAUREL and B. WATTRISSE, in IUTAM Symposium on Advanced Optical Methods and Applications in Solid Mechanics, Netherland, 2000, p. 313.
20. S. BARDET, in "Comportment thermoviscoelastique transverse du bois humide," Ph.D Thesis (Montpellier University, France, 2001) p. 49.
21. K. PERSSON, Swedish Lund University/Lund Institute of Technology Report TVSM-3020 (1997)

Received 27 September 2004
and accepted 4 January 2005